

SOLAR SEISMOLOGY. I. THE STABILITY OF THE SOLAR p -MODES*

PETER GOLDREICH

California Institute of Technology, Pasadena

AND

DOUGLAS A. KEELEY

Lick Observatory, Board of Studies in Astronomy and Astrophysics, University of California, Santa Cruz

Received 1976 April 12

ABSTRACT

We investigate the stability of the radial p -modes of the Sun by computing nonadiabatic eigenvalues and eigenfunctions for a solar envelope model which extends from an inner radius $r \approx 0.3 R_{\odot}$ out to an optical depth $\tau \approx 3 \times 10^{-4}$. Our calculations take into account in a crude fashion the response of the convective flux to the oscillation. The dynamical effect of turbulence in the convection zone is parametrized in terms of a turbulent shear viscosity.

The results of our calculations are as follows. If damping by turbulent viscosity is neglected, all modes with periods longer than 6 minutes are unstable. The familiar κ -mechanism, which operates in the H ionization-H⁻ opacity region, is the dominant source of driving of the oscillations. Modes with periods shorter than 6 minutes are stabilized by radiative damping in the solar atmosphere. When turbulent dissipation of pulsational energy is included, all modes are predicted to be stable. However, the margin of stability is very small. In view of the large uncertainty that must be assigned to our estimate of turbulent damping, we conclude that theoretical calculations cannot unequivocally resolve the question of the stability of the solar p -modes.

Subject headings: stars: pulsation — Sun: atmospheric motions — Sun: interior

I. INTRODUCTION

This is the first of a series of papers in which we survey the physical processes responsible for the excitation and damping of the normal modes of the Sun. Our aim is an ambitious one: to theoretically estimate the order of magnitude of the energy in each normal mode. One of the principal obstacles that such an investigation faces is the modeling of time-dependent convection, a task of almost legendary difficulty. Because we are not quite equal to this task, our theoretical conclusions suffer from certain ambiguities. We are guided in our attempts to resolve these ambiguities by the observations of solar oscillations.

At the present time, the observational situation regarding the existence of measurably excited normal modes is somewhat unsettled. The 5-minute oscillations of the Sun (Leighton, Noyes, and Simon 1962) have been observed by many different workers, and their existence is beyond doubt. They are most readily interpreted as excited, high-order, nonradial p - (acoustic) modes of the Sun (Ulrich 1970, Leibacher and Stein 1971, Wolff 1972). The photospheric granulation is thought to be the surface manifestation of convection and thus provides observational evidence for excited g - (gravity) modes of the Sun. The 5-min oscillations and the granulation are the only examples of well-established observational evidence for excited solar normal modes. Within the past year

three groups have claimed the detection of additional solar pulsations. Hill, Stebbins, and Brown (1975) report that the apparent diameter of the Sun is oscillating with a fractional amplitude of about 10^{-5} and that the power spectrum of these oscillations exhibits several peaks at periods shorter than 1 hour. Severny, Kotov, and Tsap (1976) and Brookes, Isaak, and van der Raay (1976) report the discovery of a 2 m s^{-1} oscillation of the solar surface with a period of 2 hr 40 min. The latter group also presents evidence for oscillations at periods of 58 min and 40 min.

In this paper we investigate the linear stability of the solar p -modes. Our calculations are restricted to radial modes. However, we expect that they provide a good indication of the stability of nonradial p -modes as well. While our study was in progress, Ando and Osaki (1975) reported the results of their investigation of p -mode stability. Their calculations are similar to ours in many respects and differ principally in that they calculate nonradial modes and do not take into account the interaction between convection and pulsation. The paper by Ando and Osaki contains a clear description of the basic equations that govern nonadiabatic oscillations. Thus we describe in detail only those aspects of our computations that differ from theirs.

The organization of this paper is as follows. In § II, we describe the solar model and the technique used to compute the eigenvalues and eigenfunctions. The effects of turbulent viscosity are modeled in § III. Then a description of the damping and driving of the modes is given in § IV. The loss of pulsational energy due to

* Contribution Number 2731 of the Division of Geological and Planetary Sciences, California Institute of Technology, Pasadena, California 91125.

the emission of a traveling wave into the corona is estimated in § V. Finally, § VI contains a comparison of our results with those obtained by other workers and also outlines the directions of future research.

II. NUMERICAL COMPUTATIONS

a) The Solar Model

Our solar envelope model is computed on a grid of 140 points, 15 of which are at optical depth $\tau \leq \frac{2}{3}$. The inner and outer boundaries of the model are at $r \approx 0.3 R_\odot$ and $\tau \approx 2.7 \times 10^{-4}$. The chemical composition is taken to be $X = 0.7054$, $Y = 0.2802$, and $Z = 0.0144$. For temperatures below 2.5×10^5 K, we adopt the opacity formula described by Christy (1966); above this temperature, we gradually replace Christy's formula by the one given in Faulkner (1966). We calculate the convective flux according to the standard mixing-length theory as formulated by Mihalas (1965) with a mixing length of 1 pressure scale-height H . The run of variables in our envelope model is quite similar to that in other solar models (e.g., Schwarzschild 1958). The dependences of the radial coordinate r , the convective velocity v_H , and the convective time scale $\tau_H = H/v_H$ on the logarithm of the pressure $\log p$ are illustrated in Figure 1. The hooks on the ends of the curves for v_H and τ_H arise because we are using a local mixing length theory.

b) The Linear Stability Calculations

We compute nonadiabatic eigenfunctions and the corresponding complex eigenvectors for radial modes by use of the inverse iteration method (Wilkinson 1955) as applied by Keeley (1977). A complete discussion of the linearized equations is given in the latter reference.

The radiative luminosity perturbation is calculated taking into account in a rough way the deviation of the mean intensity from the Planck function (integrated

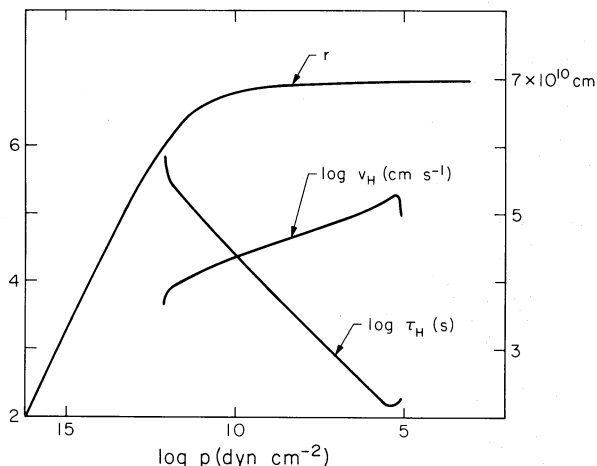


FIG. 1.—Plots of $\log v_H$, $\log \tau_H$, and r as functions of $\log p$. All quantities are expressed in cgs units. The left-hand scale refers to $\log v_H$ and $\log \tau_H$, and the right-hand scale to r .

over frequency). This procedure, which is sometimes referred to as the Eddington approximation, is described by Unno and Spiegel (1966). It has the important effect of making the luminosity eigenfunction almost constant in the optically thin region.

The time scale of the largest convective eddies ranges from approximately 10^6 s at the bottom of the convection zone to approximately 10^2 s near the top. We treat time-dependent convection according to the approach suggested by Cox *et al.* (1966). The convective luminosity satisfies the equation

$$\frac{dL}{dt} = \frac{L_0 - L}{\tau_H}, \quad (1)$$

in which L_0 is the convective luminosity given by the usual mixing-length theory and τ_H is the local convective time scale. We linearize equation (1) about the time-independent solution and obtain

$$\delta L(1 + \sigma \tau_H) = \delta L_0, \quad (2)$$

for a time dependence $\exp(\sigma t)$, where $\sigma = i\omega + \gamma$ is the eigenvalue sought in the stability analysis. We also found it desirable to include a diffusion-like term to smooth the convective luminosity perturbation over a distance of order the scale height. Further details of the treatment of time-dependent convection are discussed by Keeley (1977). The main effect of this formulation is to decrease the amplitude and shift the phase of the convective luminosity perturbation for $|\sigma \tau_H| \geq 1$. The effects of turbulent convection are not included in the momentum equation. They are computed from perturbation theory as described in § III.

The linearized equations are iterated until the real and imaginary parts of the eigenvalue are steady to 1 part in 10^9 . Typically, the eigenvector then satisfies the original difference equations to better than 1 part in 10^9 .

Because the inner boundary conditions $\delta L = 0$, $\delta r = 0$ are applied at $r = 0.3 R_\odot$, the periods obtained for the low-order radial modes are slightly too short and the radiative damping below the convective zone is underestimated. However, even for the fundamental radial mode, these effects are too small to be of great concern.

Before we proceed further, it is convenient to define some of the notation that we shall use. We have already mentioned the complex eigenvalue $\sigma \equiv i\omega + \gamma$. The velocity eigenfunctions are denoted by $v_q(r)$ and are normalized so that

$$\int_0^{M_\odot} dm' |v_q|^2 \equiv 1. \quad (3)$$

We refer to

$$M_q \equiv \frac{1}{|v_q(R_\odot)|^2} \quad (4a)$$

and

$$E_q \equiv \frac{1}{2} M_q (\omega_q R_\odot)^2 \quad (4b)$$

as the effective mass and the normalized energy of mode q . The normalization is such that the peak surface velocity is equal to $\omega_q R_\odot$. In an entirely analogous manner, we define the normalized rate of energy addition to mode q to be

$$P_q = 2\gamma_q E_q. \quad (5)$$

III. TURBULENT DAMPING IN THE CONVECTIVE ZONE

There is no sound theoretical or experimental basis from which to proceed in choosing an expression for the turbulent stress tensor. The best that we can hope to do is to estimate the magnitude of the turbulent damping by analogy with the well-understood case of molecular viscosity. For this purpose we assume that the turbulent stress may be related to the shear by a scalar coefficient of turbulent viscosity ν_t .¹ It then follows from perturbation theory that the turbulent stress makes a contribution to the normalized average rate of energy dissipation for mode q which is given by (Ledoux and Walraven 1958)

$$D_q = \frac{4}{3} E_q \int_0^{M_\odot} dm' \nu_t \left| r \frac{d}{dr} \left(\frac{v_q}{r} \right) \right|^2. \quad (6)$$

The next problem is to choose an appropriate expression for ν_t . From the picture of a turbulent flow as a superposition of eddies of different sizes, it seems plausible that only those eddies whose characteristic turnover times are significantly shorter (by a factor of order 2π) than the oscillation period will contribute to ν_t (Goldreich and Nicholson 1977). Consequently we adopt for ν_t the expressions

$$\nu_t = v_H H = v_H^2 \tau_H \quad \text{if} \quad \tau_H \omega_q < 1$$

and

$$\nu_t = v_\lambda \lambda = v_\lambda^2 \tau_\lambda \quad \text{if} \quad \tau_H \omega_q > 1. \quad (7)$$

Here H and v_H are the pressure scale-height and the convective velocity while λ and v_λ are the characteristic scale length and velocity of eddies for which $\tau_\lambda \omega_q \approx 1$. Mixing-length theory determines only v_H . In order to relate λ and v_λ to H and v_H , we must have some knowledge of the turbulent spectrum. Fortunately, the Kolmogoroff spectrum appears to be applicable in this case (cf. Appendix). Thus,

$$v_\lambda \approx v_H \left(\frac{\tau_\lambda}{\tau_H} \right)^{1/2}, \quad \lambda \approx H \left(\frac{\tau_\lambda}{\tau_H} \right)^{3/2} \quad (8)$$

is the appropriate scaling, and ν_t may be written in the more compact form

$$\nu_t = v_H^2 \tau_H \min [1, (\tau_H \omega_q)^{-2}]. \quad (9)$$

A nonperturbative calculation of the effects due to turbulent viscosity yields results that are essentially identical to those reported in this paper.

¹ Other dynamical effects due to turbulence are mentioned in §VI.

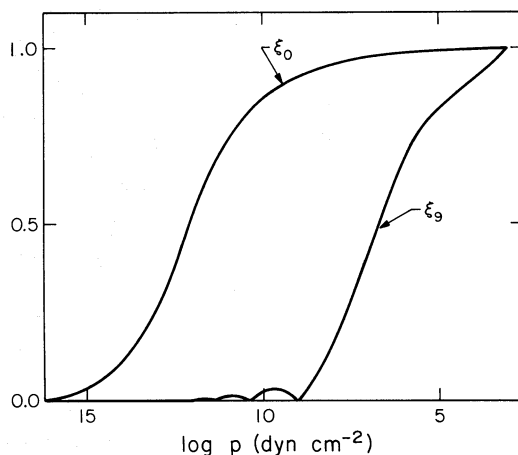


FIG. 2.—The relative radial displacement ξ for the f - and p_9 -modes is shown as a function $\log p$.

IV. DRIVING AND DAMPING

The location and strength of the sources of driving and damping depend upon the frequency of the normal mode. In order to illustrate the range of behavior exhibited by the different normal modes, we describe in detail the driving and damping of the f - and p_9 -modes.² According to our calculations, these modes have periods of 56 min and 10 min, respectively. The relative radial displacement

$$\zeta_q(r) = \frac{v_q(r) R_\odot}{v_q(R_\odot) r} \quad (10)$$

for each of the modes is illustrated in Figure 2. We see that motions associated with the higher-order mode are more strongly concentrated toward the solar surface. Figures 3 and 4 show how the contributions to the normalized average kinetic energy of each mode

² We adopt standard notation and use f and p_p ($q \geq 1$) to represent the radial modes. The subscript on the p denotes the number of nodes of the velocity eigenfunction.

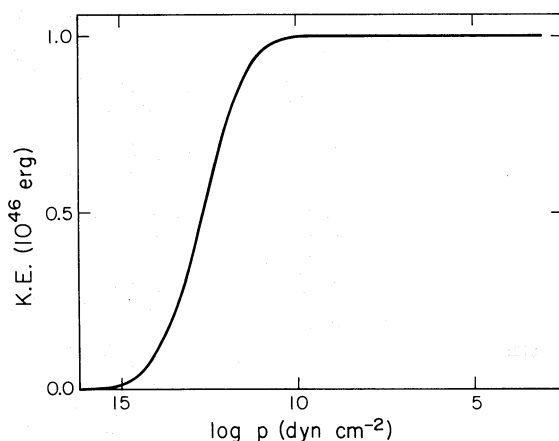


FIG. 3.—The contribution, from the bottom of the solar envelope out to pressure p , to the integral for the normalized average kinetic energy of the f -mode.

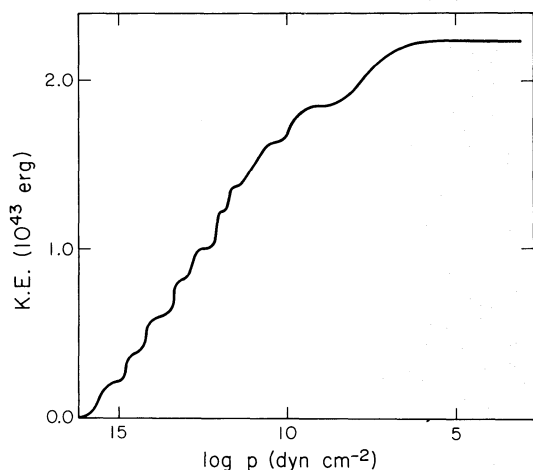


FIG. 4.—Same as Fig. 3 except for the p_9 -mode. The wiggles are due to the nodes of the velocity eigenfunction.

depend upon depth in the solar envelope. About 75% of the kinetic energy of the f -mode and 50% of the kinetic energy of the p_9 -mode are located below the convective zone ($\log p \approx 12.1$).

a) The f -Mode

The contributions to the driving and damping of the f -mode are graphed in Figure 5. From this figure we see that the model calculations predict instability if turbulent viscosity is neglected and stability if it is included. The real part of the eigenvalue for each of these two cases is $\gamma_0' = +1.06 \times 10^{-12} \text{ s}^{-1}$ and $\gamma_0 = \gamma_0' + \gamma_0'' = 4.3 \times 10^{-13} \text{ s}^{-1}$, respectively.³

The two main contributions to the driving occur at

³ Here and in future we denote by γ_q' and γ_q'' the parts of γ_q that arise from nonadiabatic effects and from turbulent viscosity, respectively.

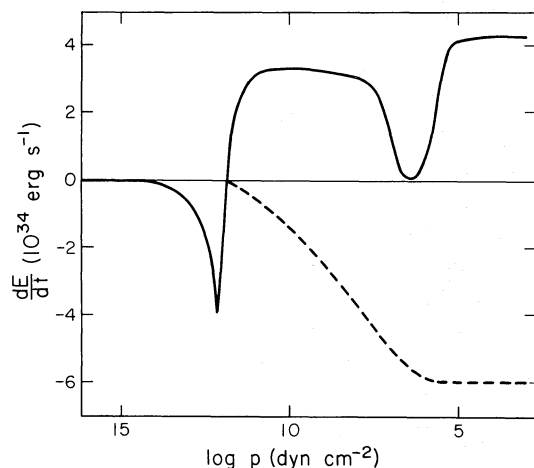


FIG. 5.—The solid line shows the integrated contribution, from the base of the solar envelope out to pressure p , to the normalized average rate of energy addition (excluding turbulent damping) to the f -mode. The dashed line gives the integrated contribution, from the base of the solar envelope out to pressure p , to the normalized average rate of turbulent energy dissipation.

the bottom of the convection zone and in the H ionization- H^- opacity region at and just above the top of the convection zone. The latter contribution is due to the κ -mechanism (Ando and Osaki 1975) which has been extensively studied in connection with the Cepheid variables (e.g., Cox and Giuli 1968). Driving occurs at the bottom of the convection zone because here the luminosity perturbation is in phase with the density perturbation and its amplitude decreases outward. Thus energy is absorbed during compression and released during expansion, the situation required for driving. The luminosity perturbation is almost entirely in the radiative portion of the luminosity because the response time of the convection is much longer than the oscillation period. Since the magnitude of the static radiative luminosity decreases outward at the bottom of the convection zone, the magnitude of its perturbation also decreases outward there. The mechanism for driving at the bottom of the convection zone has been discussed by Cox and Giuli (1968) and its presence noted in connection with numerical stability calculations by Boury *et al.* (1975).

There are three major contributions to the damping of the f -mode. Considerable damping occurs in the radiative interior just below the convection zone. Here the luminosity perturbation is in phase with the density perturbation, and its amplitude is increasing outward. Additional damping arises toward the top of the convection zone just below the H ionization- H^- opacity region. In this region $\tau_H \omega_0$ is of order unity and is decreasing outward. Thus with increasing r the luminosity perturbation, which is mainly in the convective part, is increasing in amplitude and becoming more in phase with the density perturbation. Damping due to turbulent viscosity is distributed throughout the convection zone. With increasing r , the increase in ν_t and the decrease in ρ are such that the rate of energy dissipation per unit interval in $\log p$ remains almost constant.

b) The p_9 -Mode

Figure 6 illustrates the contributions to the driving and damping of the p_9 -mode. Our model calculations predict instability if turbulent viscosity is neglected

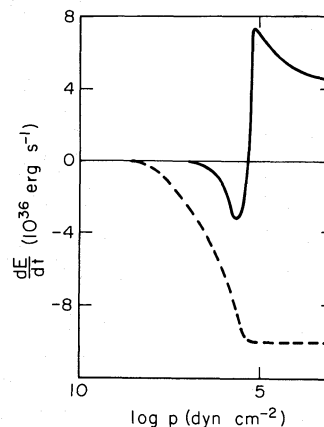


FIG. 6.—Same as Fig. 5 except for the p_9 -mode

and stability if it is included. The real part of the eigenvalue for each of these cases is $\gamma_0' = 5.1 \times 10^{-8} \text{ s}^{-1}$ and $\gamma_0 = \gamma_0' + \gamma_0'' = -6.5 \times 10^{-8} \text{ s}^{-1}$, respectively.

The principal contribution to the driving of the p_0 -mode occurs in the H ionization–H[−] opacity region. Only insignificant amounts of driving and damping occur near the bottom of and below the convection zone.

There are three significant contributions to the damping of the p_0 -mode. Considerable damping takes place just below the H ionization–H[−] opacity region where $\tau_H \omega_0$ is of order unity. Additional damping occurs in the optically thin atmospheric layers. The damping due to turbulent viscosity is concentrated in the upper part of the convective zone.

c) Generalizations regarding Driving and Damping

Except for the longest period modes (essentially only the f - and p_1 -modes), the important contributions to the driving and damping arise in the upper part of the convection zone and in the atmospheric layers. The familiar κ -mechanism, which operates in the H ionization–H[−] opacity region, is the dominant source of driving. All modes show some damping in the upper convection zone just below the driving region. This damping is confined to the region where $\tau_H \omega_0 \lesssim 1$, and its magnitude decreases relative to the magnitude of the driving with increasing modal frequency. Damping in the optically thin layers of the solar atmosphere is a consequence of their finite thermal relaxation times. Atmospheric damping is most severe for high frequency modes (Ando and Osaki 1975).

In the absence of turbulent damping, our calculations indicate instability for all radial p -modes with periods longer than 6 min. Modes whose periods are shorter than 6 min (p_q with $q \geq 18$) are stabilized by atmospheric damping. The lower limit to the periods

of the unstable modes cannot be considered a firm one since, as Ando and Osaki (1975) have shown, this limit is very sensitive to the detailed structure of the model atmosphere.

When turbulent damping is included in our calculations, all modes are predicted to be stable. However, the margin of stability is very small. For $q \leq 15$, the value of $|\gamma_q''/\gamma_q'|$ ranges from 1.4 to 5.2. This is a surprising result and one for which we have no fundamental explanation. In any case, our treatment of turbulent damping is certainly not reliable to a factor of 5. Thus our calculations are not capable of resolving the question of the stability of the radial p -modes of the Sun.

For completeness, we list in Table 1 some of the properties of the radial p -modes.

V. THE CORONAL WAVE

The normal modes of oscillation of the Sun are not pure standing waves. Even if nonadiabatic effects and turbulent viscosity were neglected, each mode would be damped by the radiation of a wave into the solar corona. Because the nonadiabatic effects and turbulent viscosity give rise to small values of γ_q , other sources of damping such as the radiation of a coronal wave must be considered.⁴ A full nonadiabatic treatment of the emission of a coronal wave would be a formidable undertaking since it would require the development of a model for the heating of the chromosphere and corona. A far more restricted problem is solved here. However, we believe that the results obtained provide a valid estimate of the damping due to the emission of the coronal wave.

We begin by adopting a hydrostatic model of the solar atmosphere which extends from the temperature

⁴ Schatzman (1956) and Unno (1965) have studied this problem in connection with the Cepheid variables.

TABLE 1
IMPORTANT PROPERTIES OF THE p -MODES

q	ω_q (s^{-1})	γ_q' (s^{-1})	γ_q'' (s^{-1})	γ_q (s^{-1})	E_q (erg)	M_p (g)
0.....	1.88(−3)	1.1(−12)	−1.5(−12)	−4.3(−13)	2.0(46)	2.3(30)
1.....	2.72(−3)	3.7(−12)	−1.4(−11)	−9.8(−12)	8.9(45)	4.9(29)
2.....	3.68(−3)	1.6(−11)	−8.5(−11)	−6.9(−11)	3.9(45)	1.2(29)
3.....	4.63(−3)	8.7(−11)	−3.9(−10)	−3.1(−10)	1.7(45)	3.2(28)
4.....	5.59(−3)	3.5(−10)	−1.3(−9)	−9.7(−10)	9.1(44)	1.2(28)
5.....	6.54(−3)	1.2(−9)	−3.9(−9)	−2.7(−9)	4.7(44)	4.5(27)
6.....	7.49(−3)	3.4(−9)	−9.7(−9)	−6.4(−9)	2.7(44)	2.0(27)
7.....	8.45(−3)	9.0(−9)	−2.3(−8)	−1.4(−8)	1.5(44)	8.6(26)
8.....	9.37(−3)	2.2(−8)	−5.3(−8)	−3.1(−8)	8.1(43)	3.8(26)
9.....	1.03(−2)	5.1(−8)	−1.2(−7)	−6.5(−8)	4.5(43)	1.7(26)
10.....	1.12(−2)	9.6(−8)	−2.2(−7)	−1.2(−7)	2.8(43)	9.1(25)
11.....	1.20(−2)	1.5(−7)	−3.4(−7)	−1.9(−7)	2.1(43)	6.0(25)
12.....	1.29(−2)	2.1(−7)	−4.9(−7)	−2.8(−7)	1.6(43)	3.9(25)
13.....	1.38(−2)	2.6(−7)	−6.8(−7)	−4.2(−7)	1.3(43)	2.8(25)
14.....	1.47(−2)	3.0(−7)	−9.3(−7)	−6.2(−7)	1.0(43)	1.9(25)
15.....	1.55(−2)	3.0(−7)	−1.2(−6)	−9.1(−7)	8.3(42)	1.4(25)
16.....	1.64(−2)	2.2(−7)	−1.5(−6)	−1.3(−6)	7.0(42)	1.1(25)
17.....	1.73(−2)	1.1(−8)	−1.7(−6)	−1.7(−6)	6.5(42)	8.9(24)
18.....	1.81(−2)	−2.9(−7)	−1.8(−6)	−2.1(−6)	6.3(42)	7.8(24)
19.....	1.89(−2)	−7.1(−7)	−2.0(−6)	−2.7(−6)	5.9(42)	6.7(24)
20.....	1.98(−2)	−1.3(−6)	−2.1(−6)	−3.4(−6)	5.5(42)	5.7(24)
21.....	2.06(−2)	−1.9(−6)	−2.1(−6)	−4.1(−6)	5.4(42)	5.2(24)

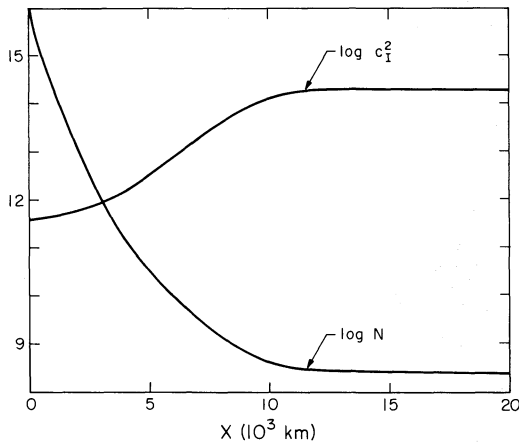


FIG. 7.—The logarithms of the square of the isothermal sound speed $c_1^2 = p/\rho$ and the total hydrogen number density N are plotted against the distance above the temperature minimum. All quantities are expressed in cgs units.

minimum to well above the base of the corona. The temperature and density profiles are obtained from the summary data compiled by Allen (1973). We have made some small adjustments to the density profile in order to make it consistent with the temperature profile and the equation of hydrostatic equilibrium. The profiles of the isothermal sound speed and the total hydrogen number density are shown in Figure 7.

We assume that the velocity perturbation satisfies the adiabatic wave equation above the temperature minimum. This equation may be written as (Ledoux and Walraven 1958)

$$\frac{d^2 v_q}{dx^2} - \frac{\Gamma g}{c^2} \frac{dv_q}{dx} + \frac{\omega_q^2}{c^2} v_q = 0, \quad (11)$$

where the plane-parallel approximation has been used and both the adiabatic index Γ and the gravitational acceleration g have been taken to be constants. The coordinate $x = r - R_\odot$, where R_\odot is the radius at the temperature minimum. The quantity $c^2 = \Gamma p/\rho$ is the adiabatic sound speed. The nature of the solutions of equation (11) is well known. Propagating waves exist for frequencies above the acoustic cutoff frequency

$$\Omega = \Gamma g/2c. \quad (12)$$

This parameter reaches its maximum value of $\Omega \approx 3.3 \times 10^{-2} \text{ s}^{-1}$ (for $\Gamma = 5/3$) at the temperature minimum. Thus modes with periods longer than about 190 s are evanescent near the temperature minimum. However, these modes tunnel through the forbidden region and emerge, with reduced strength, as traveling waves higher in the solar atmosphere.

The adiabatic approximation, on which equation (11) is based, is not justified in the solar atmosphere for the modes that we are considering. The radiative relaxation times in both the photosphere and portions of the chromosphere are shorter than the modal periods. However, we are only concerned with estimating the importance of the emission of the

coronal wave as a source of mode damping. Thus for our purpose, it is sufficient to bound the energy radiated into the corona. This may be done, within the framework provided by the adiabatic assumption, by setting $\Gamma = 1$ in equation (11) and by using the isothermal sound speed for c . Of course, we cannot rule out the possibility that a complete nonadiabatic treatment would lead to a still higher rate of energy loss. However, this possibility seems unlikely to us.

To calculate the damping produced by the emission of the coronal wave, we numerically integrate equation (11) (with $\Gamma = 1$) from $x_0 = 2 \times 10^4 \text{ km}$ to $x = 0$. The boundary condition at $x = x_0$ is determined by requiring that the solution have the form of an outward propagating wave there. Since $c = \text{constant}$ for $x \geq x_0$, this boundary condition may be obtained analytically. We find

$$\frac{dv_q}{dx} \Big|_{x=x_0} = \left\{ \frac{\Gamma g}{2c^2} + i \left[\left(\frac{\omega_q}{c} \right)^2 - \left(\frac{\Gamma g}{2c^2} \right)^2 \right] \right\} v_q(x_0). \quad (13)$$

The Eulerian pressure perturbation is related to the velocity perturbation by

$$\frac{p_q}{p} = \frac{i\Gamma}{\omega_q} \left[\frac{dv_q}{dx} - \frac{gv_q}{c^2} \right]. \quad (14)$$

If we write $v_q = \hat{v}_q \exp(i\varphi_q)$, where \hat{v}_q and φ_q are real, then it is straightforward to prove that the normalized energy flux carried by the coronal wave associated with mode q is

$$F_q = \frac{\omega_q R_\odot^2 \rho c^2}{2} \left[\frac{\hat{v}_q(x)}{\hat{v}_q(R_\odot)} \right]^2 \frac{d\varphi_q}{dx}(x). \quad (15)$$

The emission of the coronal wave makes a contribution to γ_q that is given by

$$\gamma_q'' = -\frac{2\pi R_\odot^2 F_q}{E_q}. \quad (16)$$

We have integrated equation (11) from $x = x_0$ to $x = 0$ for $\omega_q = \omega_0$ and $\omega_q = \omega_9$. The results obtained for \hat{v}_0 and \hat{v}_9 are illustrated in Figure 8. The damping rates we find are $\gamma_0'' = 1.1 \times 10^{-16} \text{ s}^{-1}$ and $\gamma_9'' = 3.3 \times 10^{-10} \text{ s}^{-1}$. These values are to be compared with the values of $\gamma_0'' = 1.48 \times 10^{-12} \text{ s}^{-1}$ and $\gamma_9'' = -1.16 \times 10^{-7} \text{ s}^{-1}$ given in Table 1. Based on this comparison, we conclude that damping due to the emission of the coronal wave is much weaker than that due to turbulent viscosity.⁵

VI. DISCUSSION AND CONCLUSIONS

a) Comparison with Other Work

As mentioned previously, the investigation of p -mode stability by Ando and Osaki (1975) has many similarities to our study. However, Ando and Osaki

⁵ This conclusion might not apply to modes with periods of order 5 min or shorter. However, a reliable calculation of the coronal wave for these modes probably requires a detailed nonadiabatic treatment which is beyond the scope of this investigation.

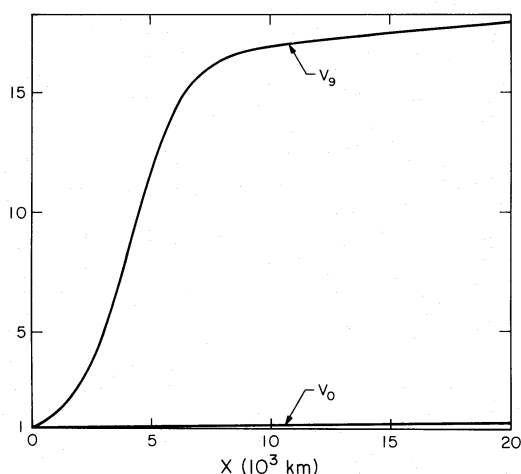


FIG. 8.—The velocity amplitudes of the coronal waves associated with the f - and p_9 -modes are shown as a function of the distance above the location of temperature minimum. The velocity amplitudes have been set equal to unity at $x = 0$.

ignore the coupling between convection and pulsation whereas we find this interaction to be of considerable importance. Aside from this major difference, our results agree fairly well with theirs. The magnitudes we compute for the growth or damping rates of the radial p -modes (neglecting damping due to turbulent viscosity) are very close to those computed by Ando and Osaki for low- l p -modes of comparable period. However, we find stronger atmospheric damping for short-period modes than they do. Thus, in the absence of turbulent damping, we predict stability for radial modes with periods shorter than 6.0 minutes whereas Ando and Osaki only predict stability for $l = 10$ modes with periods shorter than 3.8 minutes.

The stability of low-order radial and nonradial modes has also been discussed recently by Scuflaire *et al.* (1975). Their calculations differ from ours in several important respects. They use a much more detailed treatment of time-dependent convection than we do. Furthermore, they analyze complete solar interior models and account for the perturbation of the sources of nuclear energy generation. They find, for the p -modes, that the nuclear energy terms are very much less important to stability than the flux divergence terms. Another important difference is that Scuflaire *et al.* use perturbation analysis based on

adiabatic eigenfunctions to determine the growth or damping rates whereas our calculations are fully non-adiabatic. Thus they cannot include the effects that the surface region has on stability since the nonadiabatic terms are very large there. In view of the fact that the major source of driving is located near the solar surface in the H ionization-H⁻ opacity region, it is not surprising that the calculations by Scuflaire *et al.* indicate stability for the low-order p -modes.

b) Conclusions

The question of the linear stability of the solar p -modes cannot be unequivocally resolved by theoretical calculations. The principal obstacle that must be overcome is the lack of a reliable theory of time-dependent convection. The prospect that such a theory could be developed in the near future is very dim. An adequate theory would have to account not only for the time-dependence of the convective flux but also for the dynamical interaction between the turbulent convection and the large-scale fluid motions. We have parametrized this dynamical coupling by means of a coefficient of turbulent shear viscosity that we have estimated from mixing-length theory and the Kolmogoroff scaling. Clearly, this is at best an uncertain procedure. In fact, it is obvious that we have ignored several potentially significant effects. Among them are turbulent pressure, turbulent bulk viscosity, and the dissipation of turbulent energy into heat.

c) Future Research

It is possible that the question of the stability of the solar p -modes might be resolved by a comparison between theoretical predictions and observational data. To this end, we plan to estimate theoretically the energy to be expected in the p -modes on either of two hypotheses. The first hypothesis is that turbulent viscosity is sufficient to stabilize the modes. In this case, the energy in the modes should be determined by their interaction with the turbulent convection. The second hypothesis is that some of the p -modes are linearly unstable in spite of turbulent damping. In this case, the energy in each mode is probably set by its nonlinear interactions with other modes.

This research was supported by NASA grant NGL-05-002-003 and NSF grants MPS 72-05045 A02, GU-3162 and GPX-32337 X1.

APPENDIX

This appendix is intended to serve two purposes. The first is to demonstrate that the Kolmogoroff scaling is applicable to turbulent convection and to justify the choice of the coefficient of turbulent viscosity adopted in § III. The second purpose is to describe the scaling for entropy fluctuations in turbulent convection since extensive use will be made of this result in Paper II.

Kolmogoroff's picture of turbulent shear flow in an isentropic fluid is well known. The turbulent flow is considered to be composed of a hierarchy of eddies. At each scale length λ , the eddies are critically damped by turbulent viscosity due to eddies whose scale length is slightly smaller than λ . At a sufficiently small scale length λ^* , molecular viscosity becomes important and the kinetic energy of the fluid is irreversibly dissipated into heat. We are not concerned here with scales as small as λ^* , since eddies whose time scales $\tau_\lambda \approx \lambda/v_\lambda$ are comparable to the free

oscillation periods of the low-order radial modes of the Sun have length scales $\lambda \gg \lambda^*$. For $\lambda^* \ll \lambda \ll H$, where H is the largest scale in the flow, the Kolmogoroff scaling implies (Tennekes and Lumley 1972)

$$v_\lambda \approx v_H \left(\frac{\lambda}{H} \right)^{1/3} \approx v_H \left(\frac{\tau_\lambda}{\tau_H} \right)^{1/2}. \quad (\text{A1})$$

We now demonstrate that the Kolmogoroff scaling also applies to turbulent convection.⁶ This demonstration is necessary because a fluid undergoing turbulent convection possesses entropy fluctuations on all scales. The entropy fluctuations give rise to buoyancy force fluctuations which accelerate the fluid and change the kinetic energy of the eddies. However, we shall prove that, for $\lambda \ll H$, the fluctuating buoyancy force is very small compared with the fluctuating force that arises from the turbulent shear stress.

The proof is as follows. We assume that the buoyancy force is indeed negligible on scales $\lambda \ll H$. We then determine the scaling law for the entropy fluctuations from well-known results for the mixing of a passive scalar contaminant in a turbulent flow. The appropriate scaling is (Tennekes and Lumley 1972)

$$s_\lambda \approx s_H \left(\frac{\lambda}{H} \right)^{1/3} = s_H \left(\frac{\tau_\lambda}{\tau_H} \right)^{1/2}, \quad (\text{A2})$$

where s_λ is the magnitude of the entropy fluctuation of scale λ and H is the pressure scale-height which we assume to be the largest scale of the convective turbulence.⁷ The fluctuating buoyancy force per unit mass is

$$F_{b\lambda} \approx g \frac{s_\lambda}{c_v} = g \frac{s_H}{c_v} \left(\frac{\lambda}{H} \right)^{1/3}, \quad (\text{A3})$$

where c_v is the specific heat at constant volume. We can rewrite equation (A3) in a more revealing form by making use of the standard result from mixing length theory, namely,

$$v_H^2 \approx g \frac{s_H}{c_v} H. \quad (\text{A4})$$

Thus

$$F_{b\lambda} \approx \frac{v_H^2}{H} \left(\frac{\lambda}{H} \right)^{1/3}. \quad (\text{A5})$$

The corresponding expression for the fluctuating force per unit mass due to the turbulent shear stress is

$$F_{s\lambda} \approx \frac{v_\lambda^2}{\lambda} \approx \frac{v_H^2}{H} \left(\frac{H}{\lambda} \right)^{1/3}. \quad (\text{A6})$$

Comparison of the expression for $F_{b\lambda}$ and $F_{s\lambda}$ implies that for $\lambda \ll H$, the fluctuating buoyancy force does not appreciably alter either the velocity scaling given by equation (A1) or the entropy scaling given by equation (A2).

⁶ This conclusion was reached earlier by Spiegel (1962).

⁷ The entropy fluctuations give rise to temperature fluctuations that are smoothed by radiative transfer. Thus there exists a lower scale $\tilde{\lambda}$ (which in the solar convective zone is greater than λ^*) below which equation (A2) is no longer valid. However, the opacity in the solar convective zone is so high that $\tau_{\tilde{\lambda}}$ is much shorter than the periods of the low-order radial modes of the Sun. Thus equation (A2) is valid on all scales of interest to this investigation.

REFERENCES

- Allen, C. W. 1973, *Astrophysical Quantities* (3d. ed.; London: Athlone Press).
- Ando, H., and Osaki, Y. 1975, *Publ. Astr. Soc. Japan*, **27**, 581.
- Boury, A., Gabriel, M., Noels, A., Scuflaire, R., and Ledoux, P. 1975, *Astr. Ap.*, **41**, 279.
- Brookes, J. R., Isaak, G. R., and van der Raay, H. B. 1976, *Nature*, **259**, 92.
- Christy, R. F. 1966, *Ap. J.*, **144**, 108.
- Cox, J. P., Cox, A. N., Olsen, K. H., King, D. S., and Eilers, D. D. 1966, *Ap. J.*, **144**, 1038.
- Cox, J. P., and Giuli, R. T. 1968, *Principles of Stellar Structure* (New York: Gordon & Breach).
- Faulkner, J. 1966, *Ap. J.*, **144**, 978.
- Goldreich, P., and Nicholson, P. 1977, *Icarus*, in press.
- Hill, H. A., Stebbins, R. T., and Brown, T. M. 1975, *Proc. V Intern. Conf. Atomic Masses and Fundamental Constants* (Paris).
- Keeley, D. A. 1977, *Ap. J.*, **211**, 926.
- Ledoux, P., and Walraven, Th. 1958, *Handbuch der Physik*, **51**, 353.
- Leibacher, J., and Stein, R. F. 1971, *Ap. Letters*, **7**, 191.
- Leighton, R. B., Noyes, R. W., and Simon, G. W. 1962, *Ap. J.*, **135**, 474.
- Mihalas, D. 1965, *Ap. J.*, **141**, 564.
- Schatzman, E. 1956, *Contr. Inst. d'Ap. Paris*, Ser. B, No. 143.
- Schwarzschild, M. 1958, *Structure and Evolution of the Stars* (Princeton: Princeton University Press).
- Scuflaire, R., Gabriel, M., Noels, A., and Boury, A. 1975, *Astr. Ap.*, **45**, 15.
- Severny, A. B., Kotov, V. A., and Tsap, T. T. 1976, *Nature*, **259**, 87.
- Spiegel, E. A. 1962, *J. Geophys. Res.*, **67**, 3063.
- Tennekes, H., and Lumley, J. L. 1972, *A First Course in Turbulence* (Cambridge: MIT Press).

Ulrich, R. K. 1970, *Ap. J.*, **162**, 993.

Unno, W. 1965, *Publ. Astr. Soc. Japan*, **17**, 205.

Unno, W., and Spiegel, E. A. 1966, *Publ. Astr. Soc. Japan*, **18**, 85.

Wilkinson, J. H. 1955, *The Algebraic Eigenvalue Problem* (Oxford: Clarendon Press).

Wolff, C. L. 1972, *Ap. J. (Letters)*, **177**, L87.

PETER GOLDREICH: Division of Geological & Planetary Sciences, California Institute of Technology, Pasadena, CA 91125

DOUGLAS A. KEELEY: Lick Observatory, Board of Studies in Astronomy and Astrophysics, University of California, Santa Cruz, CA 95064